Available online at www.sciencedirect.com
SCIENCE DIRECT®
Inorganica Chimica Acta 344 (2003) 190–196
Inorganica Chimica Acta
www.elsevier.com/locate/ica

Synthesis and characterization of dirhodium(II,II) formamidinate complexes containing short-bite nitrogen ligands

Giuseppe Tresoldi *, Sandra Lo Schiavo, Francesco Nicolò, Paola Cardiano, Pasquale Piraino *

Dipartimento di Chimica Inorganica, Chimica Analitica e Chimica Fisica, Università di Messina, Salita Sperone n. 31, Vill. S. Agata, 98166 Messina, Italy

Received 8 July 2002; accepted 6 September 2002

Abstract

The Rh_2^{4+} complex $[Rh_2(form)_2(O_2CCF_3)_2(H_2O)_2]$ (form = *N*,*N*′-di-*p*-tolylformamidinate anion) easily reacts with the short-bite ligand pyrido[2,3-*b*]pyrazine, molar ratio 1:2, yielding the complex $[Rh_2(form)_2(pyrido[2,3\text{-}b]pyrazine)_2(O_2CCF_3)_2]$ which has been characterized by conductivity measurements and IR and ^1H NMR spectroscopy. The complex exhibits a ''lantern'' type structure with the two nitrogen ligands coordinated, in a *cisoid* arrangement, at the equatorial positions across the dirhodium unit while the axial sites are occupied by two monoligated trifluoroacetate groups. Conductivity and IR data show that in DMSO the complex undergoes dissociation of both the axial ligands leading to the species $[Rh_2(form)_2(pyrido[2,3\text{-}b]pyrazine)_2(DMSO)_2]^{2+}$. The parent compound reacts also with 2-chloro-5,7-dimethyl-1,8-naphtyridine and 2,7-dichloro-5-methyl-1,8-naphtyridine leading to $[Rh_2(form)_2(O_2CCF_3)(C_{10}H_9N_2O)(H_2O)]$ and $[Rh_2(form)_2(O_2CCF_3)(C_9H_6N_2ClO)(H_2O)]$, respectively, in which the dirhodium unit is supported by three different bridging ligands. Microanalysis, ^1H NMR and X-ray data unambiguously show that the reaction proceeds, unexpectedly, with elimination of a trifluoroacetate group and the substitution of a chlorine atom of the naphtyridine ligands by oxygen.

Keywords: Dirhodium complexes; Equatorial reactivity; Nitrogen ligands

1. Introduction

Complexes containing the Rh_2^{4+} core are the center of many experimental and theoretical studies since they represent a unique example of compounds involved in catalytic as in biological processes. Dirhodium(II,II) tetracarboxylates catalyze, in fact, the synthesis of α-hydroxycarbonyl compounds via a Rh-carbene intermediate [1], decomposition [2] and C–H insertion [3] of diazocarbonyl compounds as well as cyclization of α-diazoesters [4]. They are also able to interact with GG and AA sites on single stranded oligonucleotides [5], single stranded and duplex DNA [6] and to promote DNA photocleavage [7] while exhibiting cytostatic activity against human carcinoma [8]. The introduction of two or four anionic N-donor bidentate nitrogen ligands into the ''lantern structure'' of dirhodium(II,II) carboxylate complexes dramatically affects the redox properties of these species facilitating the thermodynamic access to mixed-valent dirhodium(II,III) [9] and charge-transfer complexes [10]. It also causes a considerable improvement in their catalytic and biological activity. As an example the complex $[Rh_2(5(S)\text{-}Mepy)_4]$ (Mepy = methyl-2-pyrrolidone-5(S)-carboxylate) and its enantiomeric form promote high enantioselectivity in intramolecular cyclopropanation of allyl diazoacetates [11], intermolecular cyclopropenation of 1-alkynes with diazoesters and diazoamides [12], in lactone synthesis via intramolecular C–H insertion [13,14]. In addition the species $[Rh_2(form)_2(O_2CCF_3)_2(H_2O)_2]$ (form = *N*,*N*′-di-*p*-tolylformamidinate anion) gives rise to a significant increase in survival time of mice bearing Ehrlich ascite or Leukaemia 1210 [15]. So the introduction into the lantern structure of ligands other than

* Corresponding author. Tel.: +39-090-676 5710; fax: +39-090-393 756.
E-mail address: tresoldi@chem.unime.it (G. Tresoldi).

0020-1693/02/$ - see front matter
PII: S0020-1693(02)01303-8

carboxylates allows a greater variation in the molecular patterns and hence the chemical reactivity of dirhodium(II,II) complexes. Recently dirhodium(II,II) complexes were also involved, as linear connectors or angular building blocks, in the synthesis of redox-active square molecular boxes [16].

Following our interest in the chemistry of Rh_2^{4+} complexes we focused our attention on the synthesis of dirhodium(II,II) complexes in which the Rh_2^{4+} core is supported by nitrogen containing ligands only. We wish to report on the reaction of the complex $[Rh_2(form)_2(O_2CCF_3)_2(H_2O)_2]$ (**1**) with the short-bite nitrogen ligands pyrido[2,3-*b*]pyrazine, 2-chloro-5,7-dimethyl-1,8-naphtyridine (chloronaphy) and 2,7-dichloro-5-methyl-1,8-naphtyridine (dichloronaphy) (Fig. 1). The parent complex is an ideal starting material for the synthesis of eight-nitrogen coordinated dirhodium(II,II) complexes since the trifluoroacetate groups are very labile owing to the *trans* labilizing effect of the formamidinate groups. So complex **1** exhibits, besides the well known axial reactivity, a remarkable equatorial reactivity too. This leads to mild conditions for the coordination of bidentate ligands at the equatorial position, being completely unaffected by the $Rh(form)_2Rh$ fragment. We report also on the X-ray analysis of the complex $[Rh_2(form)_2(O_2CCF_3)(C_{10}H_9N_2O)(H_2O)]$, a rare example of a dirhodium(II,II) complex in which the Rh_2^{4+} core is supported by three different bridging ligands.

2. Results and discussion

Treatment of the complex $[Rh_2(form)_2(O_2CCF_3)_2(H_2O)_2]$ (**1**) with pyrido[2,3-*b*]pyrazine, molar ratio 1:2, yields, after minimum work-up, the green complex $[Rh_2(form)_2(pyrido[2,3\text{-}b]pyrazine)_2(O_2CCF_3)_2]$ (**2a**). The complex is an air-stable crystalline solid for which satisfactory analytical data have been obtained. The ^1H NMR ($CDCl_3$, r.t.) shows the expected signals of the methyl and methyne protons of the formamidinate fragments, as single resonances, at 2.23(s) and 7.43(t) ppm pointing out the symmetric arrangement of the two formamidinates across the Rh_2^{4+} core. Inspection of the pyridyl protons region clearly shows five sets of resonances with the right integral ratio. In particular the spectrum experiences the significant downfield shift of the H(2) (10.19 ppm) and H(7) (10.14 ppm) with respect to the corresponding values exhibited by free pyrido[2,3-*b*]pyrazine (9.07 and 9.21 ppm, respectively). On the contrary the H(3) proton, which could be affected by the N(4) coordination, is virtually unchanged.

Although pyrido[2,3-*b*]pyrazine in principle may act as a "short bite" or exobidentate ligand, the downfield shift of the H(2) and H(7) protons, very likely due the magnetic anisotropy of the rhodium centers, indicates that the nitrogen atoms N(1) and N(8) are involved in coordination. So the ligands prefer to adopt the N(1),N(8) bridging coordination mode across the dirhodium core with consequent displacement of the two trifluoroacetate groups from the equatorial sites.

Complex **2a**, which is soluble only in polar organic solvents, is non conducting in dichloromethane while in acetonitrile it behaves as a 1:2 electrolyte displaying a value of 260 Ω^{-1} cm^2 mol^{-1}. Solid IR spectrum of **2a** shows, in addition to the bands associated to the formamidine linkages, an absorption at 1668 cm^{-1} consistent with the presence of monodentate fluorocarboxylate groups, σ-coordinated at the axial positions. The occurrence of a single ν(CO) band in the solid IR spectrum suggests that both trifluoroacetates are coordinated in a similar manner. IR spectra also reveal that the compound adopts in solution a different configuration, being the ν(CO) absorption detected in CH_3CN or DMSO at 1695 cm^{-1}. The combined conductivity and IR data suggest that in coordinating solvents the monoaxial ligated trifluoroacetate groups are displaced from the axial sites and the ionic bis-adducts $[Rh_2(form)_2(pyrido[2,3\text{-}b]pyrazine)_2(L)_2]^{2+}$ ($L = CH_3CN$, DMSO) are generated [17]. The adduct $[Rh_2(form)_2(C_7H_5N_3)_2(DMSO)_2][O_2CCF_3]_2 \cdot DMSO$ (**2b**) (Fig. 2) was isolated as an air-stable crystalline solid for which satisfactory analytical data have been obtained but data from crystal of **2b** did not allow complete refinement. Notwithstanding the bad quality

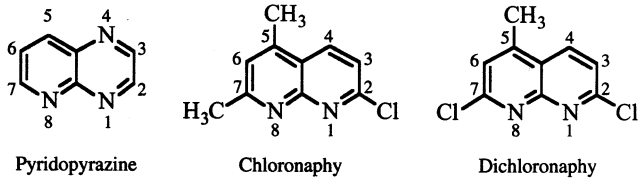

Fig. 1.

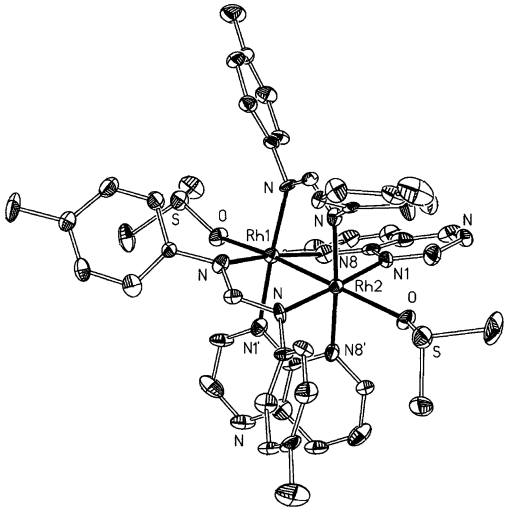

Fig. 2. Proposed structure for **2b**.

of crystal data the structure depicted in Fig. 2 is clearly detected.[1]

When the pyrido[2,3-*b*]pyrazine is allowed to react with the tetracarboxylate complex $[Rh_2(acetate)_4]$, a red–orange insoluble material, which could not to be fully characterized, was obtained. The material, which analyses as $[Rh_2(acetate)_4(pyrido[2,3\text{-}b]pyrazine)]$ (**3**), very likely corresponds to one dimensional linear chains of $Rh_2(acetate)_4$ fragments linked by the pyrido[2,3-*b*]pyrazine ligand, axially coordinated to the dirhodium units through N(1), N(4) or N(8), N(4) atoms. So it acts as an exobidentate ligand. Similar structures have been reported for the complexes $[Rh_2(acetate)_4L]$ (L = 2,3,5,6-tetramethylbenzene-1,4-diammine or phenazine) [18] and $[Rh_2(form)_2(O_2CCF_3)_2L]$ (L = pyrazine or 4,4-bipyridine) [19].

Addition of chloronaphy to a diethyl ether solution of **1** yields, after the workup described in Section 3, a yellow–brown microcrystalline solid which corresponds to the empirical formula $[Rh_2(form)_2(O_2CCF_3)(C_{10}H_9N_2O)(H_2O)]$ (**4**). Unexpectedly the microanalytical data show that the crystals contain only a trifluoroacetate group for dimeric unit and an oxygen atom has replaced a chloro group of the naphtyridine. Infrared and ^1H NMR spectra were not of much help in solving this problem but they were useful to suggest the structure further confirmed by the X-ray analysis. Complex **4**, which is non-electrolyte even in coordinating solvents, experiences the ν(CO) absorption at 1641 cm^{-1}, the value being consistent with those of bridging trifluoroacetate groups while the ^1H NMR spectra give a clear indication of the coordination mode of chloronaphy. It is worth mentioning that 1,8 naphtyridines display geometries ranging from monodentate, chelating bidentate and bridging bidentate [19], being its ability to act in a bridging bidentate mode favored by the presence of functional groups in positions 2 and 7 [20]. The ^1H NMR spectrum of **4** shows four different signals for the methyl protons (2.13, 2.23, 2.28, and 2.37 ppm) and two for the methyne protons (7.8 and 6.98 ppm) of formamidinate fragments [21], as expected for a low symmetry molecule. The methyl protons region (Table 1) also experiences two singlets at 3.01 and 2.50 ppm assigned to Me(7) and Me(5) of chloronaphy, respectively. Both the signals are downfield shifted with respect to those of uncoordinated chloronaphy (2.66 and 2.73 ppm) strongly suggesting that N(8) is involved in the coordination to the dimetal center. The analysis of the chloronaphy protons clearly shows that H(6) proton is poorly affected by the coordination while H(3) and H(4) lie at high field compared to the signals of the free ligand. The upfield shift of H(3) and H(4) protons may be due to increased shielding of the protons, caused by back-donation from dp orbitals of the metal to π^* orbitals of the ligands, as well as from the substitution of a chlorine atom by an oxygen. The combined IR and ^1H NMR data are consistent with a Rh–Rh unit supported by two *cis* formamidinate groups, one bridging trifluoroacetate and the naphtyridine bridged to the dimetal core through the N1 and N8 atoms.

When the reaction is performed by using dichloronaphy, the compound $[Rh_2(form)_2(O_2CCF_3)(C_9H_6N_2ClO)(H_2O)]$ (**5**), similar to **4**, is obtained. Once again microanalytical data confirm that the reaction proceeds with elimination of a trifluoroacetate group and substitution of a chlorine of dichloronaphy by an oxygen atom. Conductivity measurements, spectroscopic ^1H NMR and IR data suggest that a similar structure can be envisaged for **4** and **5**. The ^1H NMR spectrum of **5**, which is non-conducting, exhibits four different ^1H NMR signals for the methyl protons of the formamidinate fragment pointing out the asymmetrical arrangement of the two formamidinate ligands around the dirhodium core. Furthermore the protons of the dichloronaphy ring resonate at frequencies comparable to those detected for the chloronaphy ring of **4** (Table 1), supporting the bridging N(1)–N(8) coordination of dichloronaphy.

The reaction leading to **4** and **5** takes place with an obscure course and we do not feel confident in making unsupported speculations. We can only exclude that the formation of **4** may be caused by 5,7-dimethyl-2-hydroxy-1,8-naphtyridine (OHnaphy) impurities present in the chloronaphy because its purity has been carefully checked. Furthermore from the 1:1 reaction of **1** with Ohnaphy we recovered a mixture of products that we were unable to isolate in a pure form **4**.

We suggest that, as previously found [16–20], the first step of the reaction consists in the coordination of chloronaphy at the axial site of the dirhodium unit followed by axial–equatorial isomerization and consequent displacement of one trifluoroacetate group from the equatorial to the axial site. So a mixture of isomers is not unexpected bearing also in mind that OHnaphy may act as a bridge through N(1) and the oxygen atom. It is worth mentioning that the complex $Rh_2(O_2CCH_3)_4$, that does not exhibit equatorial reaction, reacts with OHnaphy leading to the bis axial adduct $Rh_2(O_2CCH_3)_4(OHnaphy)_2$ [22].

2.1. X-ray structure of $[Rh_2(form)_2(O_2CCF_3)(C_{10}H_9N_2O)(H_2O)]\cdot\frac{1}{2}(C_4H_{10}O)$ (4)

The molecular structure of **4**, including the atomic numbering scheme, is illustrated in Fig. 3. Selected bond distances and angles are listed in Table 2. The crystal

[1] Unpublished structural analysis of **2b** gave Rh(1)–O = 2.263(9), Rh(2)–O = 2.335(9), Rh(1)–N(1′) = 2.073(12), Rh(1)–N(8) = 2.068(11), Rh(2)–N(8′) = 2.066(11), Rh(2)–N(1) = 2.077(11).

Table 1
^{1}H NMR chemical shifts (ppm) and coupling constants (Hz)

	H(3)	H(4)	H(6)	Me(5)	Me(7)
Chloronaphy	7.43(d, $J = 8.60$)	8.24(d)	7.21(s)	2.66	2.73
Dichloronaphy	7.51(d, $J = 9.20$)	8.28(d)	7.34(s)	2.70	
OHnaphy	6.66(d, $J = 10.50$)	7.87(d)	6.89(s)	2.50	2.60
4	6.09(d, $J = 8.01$)	7.06(d)	7.05(s)	2.50	3.01
5	6.22(d, $J = 8.37$)	7.13(d)	7.00(s)	2.54	

structure is constituted by the co-crystallization of discrete molecules $[Rh_2(form)_2(O_2CCF_3)(C_{10}H_9N_2O)(H_2O)]$ with diethyl–ether in the ratio 2:1. The isolated solvent molecule is placed at a crystallographic center of symmetry and its alkyl branches are very disordered. The complex consists of a dirhodium(II) unit bridged by three different type of ligands (two adjacent formamidinates (form), one trifluoracetate and one naphthyridine derivative) while a water molecule is bound to one Rh center on the axial position. Therefore the Rh_2^{4+} unit is asymmetric and shows a distorted octahedral coordination of Rh(1) and a square pyramidal arrangement for Rh(2) having the axial site empty, while each metal carries +2 formal charge. The different surroundings have a significant influence on the corresponding coordination shell: while $Rh–O_{acet}$ distances are similar (2.095(4) vs. 2.094(4) Å), the $Rh–N_{form}$ (2.029(5) and 2.017(5) vs. 2.026(5) and 1.994(5) Å, respectively) and the $Rh–N_{naph}$ bond lengths (2.108(5) vs. 2.030(5) Å) show an elongation balancing the electronic and steric effects of the higher coordination. Whereas the formamidinate bites are symmetric and equal (the average values are C–N = 1.320(7) and N···N = 2.337(8) Å), both the $Rh–N_{form}$ distances of

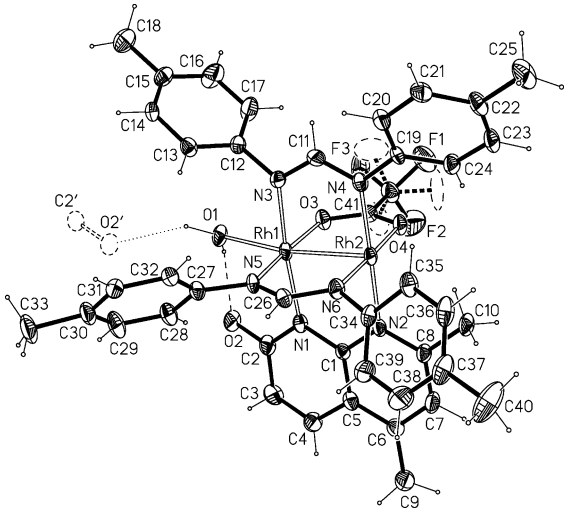

Fig. 3. Perspective view and atom numbering scheme of molecule **4**. Thermal ellipsoids are drawn at 25% of probability, while H size is arbitrary. Dashed and dotted lines represent intra- and inter-molecular (sym. op. $-x$, $-y$, $1-z$) H interactions. The co-crystallized diethyl-ether molecule has been omitted for clarity.

Table 2
Selected bond lengths (Å) and angles (°) for **4**

Bond lengths (Å)			
Rh(1)–O(1)	2.186(4)	Rh(2)–Rh(1)	2.4487(9)
Rh(1)–N(5)	2.017(5)	Rh(2)–N(6)	1.994(5)
Rh(1)–N(3)	2.029(5)	Rh(2)–N(4)	2.026(5)
Rh(1)–O(3)	2.095(4)	Rh(2)–O(4)	2.094(4)
Rh(1)–N(1)	2.108(5)	Rh(2)–N(2)	2.030(5)
N(1)–C(2)	1.384(7)	N(1)–C(1)	1.388(7)
C(1)–N(2)	1.380(7)	N(2)–C(8)	1.347(7)
C(2)–O(2)	1.260(7)	N(3)–C(11)	1.323(7)
N(3)–C(12)	1.435(7)	C(11)–N(4)	1.315(7)
N(4)–C(19)	1.425(7)	N(5)–C(26)	1.320(7)
N(5)–C(27)	1.432(7)	C(26)–N(6)	1.329(7)
N(6)–C(34)	1.430(7)	O(3)–C(41)	1.254(7)
C(41)–O(4)	1.273(7)		
Bond angles (°)			
N(5)–Rh(1)–N(3)	90.6(2)	N(3)–Rh(1)–O(3)	88.6(2)
N(5)–Rh(1)–N(1)	90.0(2)	O(3)–Rh(1)–N(1)	90.3(2)
N(5)–Rh(1)–O(1)	101.2(2)	N(3)–Rh(1)–O(1)	87.7(2)
O(3)–Rh(1)–O(1)	83.5(2)	N(1)–Rh(1)–O(1)	97.2(2)
N(6)–Rh(2)–N(4)	91.4(2)	N(6)–Rh(2)–N(2)	88.6(2)
N(4)–Rh(2)–O(4)	89.4(2)	N(2)–Rh(2)–O(4)	90.5(2)
N(2)–C(1)–N(1)	115.9(5)	N(4)–C(11)–N(3)	124.3(6)
N(5)–C(26)–N(6)	124.1(6)	O(3)–C(41)–O(4)	127.4(6)

Hydrogen bonds				
DHA	d(D–H)	d(H···A)	d(D···A)	D–H···A
O(1)–H(1A)···O(2)	0.94	1.91	2.517(6)	119.7
O(1)–H(1B)···O(2)′	0.94	2.17	3.022(5)	149.5

The equivalent position of atom O(2) is obtained by $-x$, $-y$, $1-z$ symmetry operation.

the formamidinate *trans* to the trifluoracetate are slightly shorter than the corresponding ones of the other bridge opposite to the naphthyridine, due to the different *trans*-effect.

The bond lengths within the naphtyridine ring are irregular while the distance from C(2) to the alleged O(2) [1.252(7) Å] is very short and far from the usual

$C_{aromatic}$–O single bond distance of ~1.38 Å. These data may be explained assuming that the *exo*-cyclic O(2), involved in the conjugation with the naphtyridine system, exhibits a predominant pyridone character. The C(2)–O(2) bond length, although larger than the value of 1.233(6) found in the dirhodium (II,II) complex $Rh_2(O_2CCH_3)_4(OHnaphy)_2$ [22], denotes a high percentage of double bond. A study on all the 69 1,8-naphthyridine-2-oxo fragments reported in the CSD [23] has evidenced bond length values ranging from 1.21(3) [24] up to 1.37(1) Å [25] without any clear correlation between the geometry of the bicyclical ring and the delocalization degree of the double-bond. The oxygen atom O(2) is located at a very short distance [2.517(6)] from the oxygen O(1) of the axially coordinated water molecule (intramolecular hydrogen interaction, see Table 2) and simultaneously has relatively short interactions of 3.022(5) to the axially coordinated water molecule of a neighboring unit (intermolecular hydrogen interaction). The steric hindrance of the axial water molecule with the surrounding phenyl group and the naphthyridine oxygen push O(1) toward the acetate side as evidenced by the enlargement of the angles N(5)–Rh(1)–O(1) = 101.2(2) and N(1)–Rh(1)–O(1) = 97.2(2)° as compared to the contraction of O(3)–Rh(1)–O(1) up to 83.5(2)°. This hindrance might be related to the different rotation of the phenyl rings of the formamidinate: in the bridge opposite to the acetate the two *p*-tolyl groups are equally rotated with respect to the bite plane [C(26)–N(5)–C(27)–C(32) = 44.6(8) and C(26)–N(6)–C(34)–C(39) = 48.9(9)°] while in the adjacent formamidinate the ring close to the axial water is more rotated than the other one [C(11)–N(3)–C(12)–C(17) = 68.9(8) vs. C(11)–N(4)–C(19)–C(20) = 32.7(9)°]. In fact the distorsion of the Rh(1) coordination geometry is also evidenced by the 0.370(4) Å deviation of O(1) on the acetate side from the mean plane passing through the Rh_2^{4+} unit and the bite of the naphthyridine and of the opposite formamidinate bridge. However both the formamidinate bites are almost flat as evidenced by the corresponding torsion angles N–Rh–Rh–N being close to 0°, while in other $Rh_2(form)_4$ complexes the ligand torsion along the intermetallic axis is significant [10].

The Rh–Rh bond length of 2.4487(9) Å is comparable with that [2.434(1) Å] found in the homoleptic tetraformamidinate complex $[Rh_2(form)_4]$ [9b] but longer than those detected in the complexes $[Rh_2(form)_2(O_2CCF_3)_2(H_2O)_2]$ [9a] and $[Rh_2(O_2CCF_3)_2(H_2O)_2]$ [26] (2.426(1) and 2.394(3) Å, respectively). Being the Rh–Rh separation dependent on the number and the bite size of the bridges, the above data may be explained taking into account that the bite of the naphthyridine and the two formamidinate in **4** are almost similar (N···N is 2.347(8) vs. the average 2.336(8) Å, respectively) while both are significantly larger than O···O separation (2.266(7) Å) of the unique acetate bridge. In keeping a light longer inter-metallic distance [2.453(1) Å] was detected for the analogous *cis* complex $[Rh_2(form)_2(C_7H_5N_3)_2(DMSO)_2][O_2CCF_3]_2DMSO$ (**2b**) (DMSO = dimethylsulfoxide, axial coordinated via the O-atom) where both the acetate were replaced by the pyrido[2,3-*b*]pyrazine. Although the X-ray diffraction data were very bad and the model refinement did not reach a good enough level to being published, due to the very high disorder of the counter-ion trifluoracetate and the co-crystallized DMSO molecules in the crystal packing,[1] the cationic complex is sufficiently well-defined to evidence the significant agreement of its geometry with that of compound **4**.

3. Experimental

3.1. General remarks

The starting complex $[Rh_2(form)_2(CF_3COO)_2(H_2O)_2]$ [9a], 5,7-dimethyl-2-chloro-1,8-naphtyridine (chloronaphy) and 2,7-dichloro-5-methyl-1,8-naphtyridine (dichloronaphy) and 5,7-dimethyl-2-hydroxy-1,8-naphtyridine were prepared according to literature data [27] and their purity checked by elemental analysis and ^1H NMR spectra. All other chemicals are commercially available and used as supplied. None of the compounds here reported are air sensitive, but all reactions were carried out under an atmosphere of dry nitrogen. Elemental analyses were performed by REDOX snc Laboratorio di Microanalisi, Cologno Monzese (Milano), Italy. Infrared spectra were recorded on KBr pellets with a Perkin–Elmer FT 1720X spectrometer. The NMR measurements were performed with a Bruker AMX 300 spectrometer using standard pulse sequences.

3.2. Preparations

3.2.1. $[Rh_2(form)_2(C_7H_5N_3)_2(O_2CCF_3)_2]$ (**2a**)

Solid pyrido[2,3-*b*]pyrazine (0.047 g, 0.36 mmol) was added to a benzene solution (20 ml) of $[Rh_2(form)_2(CF_3COO)_2(H_2O)_2]$ (**1**) (0.160 g, 0.175 mmol) and the resulting dark-green solution was left to stir for approximately 4 h. After this time the solution was filtered and the solvent removed in vacuo affording a green solid that was recrystallized from $CHCl_3$/*n*-heptane affording **2a** as green crystals. Yield 85%. *Anal*. Found: C, 50.30; H, 3.51; N, 12.30; F, 10.05. Calc. for $C_{48}H_{40}F_6N_{10}O_4Rh_2$ (1140.72): C, 50.54; H, 3.53; N, 12.28; F, 9.99%. Λ_M (CH_3CN, 10^{-3} mol dm^{-3}, 20 °C) = 260 Ω^{-1} cm^2 mol^{-1}. IR (nujol mulls, cm^{-1}): 1577s [ν(NCN)], 1668vs [$\nu_{asym}(CO_2)$]; IR (CH_3CN, cm^{-1}): 1695vs [$\nu_{asym}(CO_2)$]. ^1H NMR ($CDCl_3$, 300.13 MHz): δ = 2.23 [s, 12H, Me(form)], 7.43 (t, $^3J_{HRh}$ = 3.6

Hz, 2H, [CH(form)], 7.78 (m, br, H6), 8.50 (dd, $^3J = 6.2$ Hz, $^4J = 1.9$ Hz, H5), 8.89 (d, H3), 10.14 (dd, $^3J = 6.2$ Hz, $^4J = 1.9$ Hz, H7), 10.19 (d, $^3J = 2.6$ Hz, H2).

3.2.2. *[Rh$_2$(form)$_2$(C$_7$H$_5$N$_3$)$_2$(DMSO)$_2$][O$_2$CCF$_3$]$_2$·DMSO (**2b**)*

2a (0.114g, 0.1 mmol) was dissolved in 20 ml of $CHCl_3$/*n*-heptane solution (1/1) in the presence of 0.5 ml of DMSO. After a few days, the green crystalline product was collected and dried in air. Yield 90%. *Anal*. Found: C, 47.00; H, 4.30; N, 10.20; F, 8.20. Calc. for $C_{54}H_{58}F_6N_{10}O_7Rh_2S_3$ (1375.12): C, 47.17; H, 4.25; N, 10.19; F, 8.29%. IR (DMSO, cm^{-1}): 1695vs [$\nu_{asym}(CO_2)$].

3.2.2.1. *[Rh$_2$(O$_2$CCH$_3$)$_4$(C$_7$H$_5$N$_3$)] (**3**).*

$[Rh_2(O_2CCH_3)_4]$ (0.108 g, 0.488 mmol) was dissolved in 30 ml of an acetone/water solution (1/1) and to the resulting mixture was added 0.064 g (0.488 mmol) of crude pyrido[2,3-*b*]pyrazine. The starting light-blue solution immediately turned green. It was left under stirring for approximately 3 h, during which time **3** precipitated as a rust solid. This was separated by filtration, washed several times with water and dried in vacuo. Yield 80%. *Anal*. Found: C, 31.24; H, 3.10; N, 7.35. Calc. for $C_{15}H_{17}N_3O_8Rh_2$ (573.13): C, 31.43; H, 2.99; N, 7.33%. IR (nujol mulls, cm^{-1}): 1561vs [$\nu_{asym}(CO_2)$].

3.2.3. *[Rh$_2$(form)$_2$(O$_2$CCF$_3$)(C$_{10}$H$_9$N$_2$O)(H$_2$O)] (**4**)*

A diethyl ether solution (20 ml) of 5,7-dimethyl-2-chloro-1,8-naphtyridine (0.021 g, 0.110 mmol) was added to a solution of **1** (0.100 g, 0.109 mmol) in the same solvent (30 ml). The resulting green-shining solution was left standing overnight, during which time a small amount of an unidentified green precipitate was formed. This was removed by filtration and the mother liquors were taken to dryness in vacuo. The dark green residue, dissolved in $CHCl_3$ (30 ml), by the time turns dark yellow and by addition of *n*-heptane (20 ml) affords compound **4** as a brown–yellow crystalline solid. Yield 63%. *Anal*. Found: C, 53.00; H, 4.53; N, 8.59; F, 6.00. Calc. for $C_{42}H_{41}F_3N_6O_4Rh_2$ (956.65): C, 52.73; H, 4.32; N, 8.78; F, 5.96%. IR (nujol mulls, cm^{-1}): 1577s [ν(NCN)], 1641vs [$\nu_{asym}(CO_2)$]. ^{1}H NMR ($CDCl_3$, 300.13 MHz): $\delta = 2.13$, 2.23, 2.28, 2.37 [4 s, 12 H, Me(form)], 6.98, 7.8 [2 t, br, 2 H, CH(form)].

3.2.4. *[Rh$_2$(form)$_2$(O$_2$CCF$_3$)(C$_9$H$_6$N$_2$ClO)(H$_2$O)] (**5**)*

A diethyl ether solution (40 ml) of 2,7-dichloro-5-methyl-1,8-naphtyridine (0.040 g, 0.188 mmol) was added to a solution of **1** (0.172 g, 0.187 mmol) in the same solvent (30 ml). From the resulting solution, left standing overnight, a light green solid precipitated. The mother liquors were pipetted off and left to evaporate at the air. After approximately 24 h a red solid was formed. It was recrystallized from $CHCl_3$/*n*-heptane affording **5** as dark red microcrystals. Yield 78%. *Anal*. Found: C, 50.38; H, 3.90; N, 8.58; Cl, 3.70. Calc. for $C_{41}H_{38}ClF_3N_6O_4Rh_2$ (977.06): C, 50.40; H, 3.92; N, 8.60; Cl, 3.63%. IR (nujol mulls, cm^{-1}): 1577s [ν(NCN)], 1645vs [$\nu_{asym}(CO_2)$]. ^{1}H NMR ($CDCl_3$, 300.13 MHz): $\delta = 2.24$, 2.29, 2.38, 2.46 [4 s, 12H, Me(form)], 7.80 [t, $^3J_{HRh} = 3.5$ Hz, 2H, CH(form)], 7.28 [t, $^3J_{HRh} = 3.7$ Hz, 2H, CH(form)].

3.2.5. *X-ray crystallographic study*

Suitable crystals of **4** were obtained by addition of *n*-heptane to a chloroform/diethyl ether solution of the compound. Single-crystal X-ray diffraction measurements were performed at room temperature on a Siemens P4 automatic four-circle diffractometer using graphite-monochromatized Mo Kα radiation ($\lambda_{MoK\alpha}$ = 0.71073 Å).

*3.2.5.1. Crystal data of **4**.* $(C_{42}H_{41}F_3N_6O_4Rh_2)\cdot\frac{1}{2}(C_4H_{10}O)$, triclinic, space group $P\bar{1}$, $a = 11.043(3)$, $b = 11.969(4)$, $c = 17.093(5)$ Å, $\alpha = 105.76(3)$, $\beta = 101.45(2)$, $\gamma = 90.78(3)^\circ$, $U = 2126(1)$ Å^3, $Z = 2$, Dcalc = 1.533 Mg m^{-3}, crystal dimensions $0.12 \times 0.10 \times 0.07$ mm, λ(Mo Kα) = 0.841 mm^{-1}, $R_1 = 0.0450/0.0976$ and $wR_2 = 0.0870/0.0973$ for 3951 (obs with $I > 2\sigma(I)$)/7533 (all the independent) reflections, goodness-of-fit = 0.776, $T = 298(2)$ K. Lattice parameters were obtained from least-squares refinement of the setting angles of 30 reflections within $12 \leq 2\theta \leq 29^\circ$ range. No crystal decay was evidenced by the measurement of three standard reflections, monitored every 197 measurements. The intensities of the 8169 reflections (collected up to $2\theta = 50^\circ$) were evaluated by a learnt-profile-fitting procedure [28] among 2θ shells and then corrected for Lorentz-polarization and absorption (semi-empirical method by azimuthal scan data [29]: min. and max. transmission factors were 0.742 and 0.900) effects. No account was taken for extinction effects. The structure was solved by standard methods and subsequently completed by a combination of least-squares technique and Fourier Syntheses. Data-collection and reduction has been performed by using the SHELXTL 5.05 system. All non-hydrogen atoms were refined anisotropically. Whereas the final difference Fourier maps showed several hydrogen positions, H atoms were placed in calculated positions (the idealized geometry depending on the parent atom type) and included in the refinement among the ''riding model'' method. The coordinated H_2O molecule has been treated as a ''rigid body'' fragment whose position has been optimized by the model refinement lsq-cycles. The terminal trifluoromethyl of the acetate bridge appeared to be affected by rotational disorder and it was restrained and split into two orientations with 0.6 and 0.4 of occupancy, respectively.

Further large electron residuals were localized around the crystallographic center of symmetry on the ΔF maps and were accounted for a very disordered diethylether molecule. The oxygen atom lies in special position and its ethyl fragment is split into two conformations of 0.5 occupancy and their geometries have to be restrained during the refinement. The model optimization was carried out by minimizing the function $\Sigma w(F_o^2-F_c^2)^2$ with the full-matrix least-square technique based on all 7533 independent F^2 [$R_{int}=0.0202$] with SHELXL97 program [30]. The last difference map showed no significant electron density residuals (ranging from -0.758 to 0.616 e $Å^{-3}$). Neutral-atom scattering factors and anomalous dispersion corrections are those included in the program [31]. Final geometrical calculations and drawings were carried out with the PARST program [32] and the XPW utility of the Siemens package, respectively.

4. Supplementary material

Crystallographic data (excluding structure factors) for the structure reported in this paper have been deposited with the Cambridge Crystallographic Data Centre, CCDC No. 181823. Copies of this information may be obtained free of charge from The Director, CCDC, 12 Union Road, Cambridge CB2 1EZ, UK (fax: +44-1223-336-033; e-mail: deposit@ccdc.cam.ac.uk or www: http://www.ccdc.cam.ac.uk).

Acknowledgements

This work was supported by the Consiglio Nazionale delle ricerche (CNR) and Ministero dell'Università e della Ricerca Scientifica e Tecnologica (MIUR) of Italy.

References

[1] J.L. Wood, G.A. Moniz, D.A. Pflum, B.M. Stoltz, A. Holubec, H.J. Dietrich, J. Am. Chem. Soc. 121 (1999) 1748.
[2] P. Manitto, D. Monti, S. Zanzola, G. Speranza, Chem. Commun. (1999) 543.
[3] D.F. Taber, K.K. You, A.L. Rheingold, J. Am. Chem. Soc. 118 (1996) 547.
[4] M. Kennedy, M.A. Mckervey, A.R. Maguire, J.H. Ross, Chem. Commun. (1990) 361.
[5] J.M. Asara, J.S. Hess, E. Lozada, K.R. Dunbar, J. Allison, J. Am. Chem. Soc. 122 (2000) 8.
[6] (a) K.V. Catalan, J.S. Hess, M.M. Maloney, D.J. Mindiola, D.L. Ward, K.R. Dunbar, Inorg. Chem. 38 (1999) 3904;
(b) K.V. Catalan, D.J. Mindiola, D.L. Ward, K.R. Dunbar, Inorg. Chem. 36 (1997) 2458.
[7] P.K.L. Fu, P.M. Bradley, C. Turro, Inorg. Chem. 40 (2001) 2476.
[8] M. Bien, F.P. Pruchnick, A. Seniuk, T.M. Lachowitz, P. Jakimowicz, J. Inorg. Biochem. 73 (1999) 45.
[9] (a) P. Piraino, G. Bruno, S. Lo Schiavo, F. Laschi, P. Zanello, Inorg. Chem. 26 (1987) 91;
(b) P. Piraino, G. Bruno, S. Lo Schiavo, F. Laschi, P. Zanello, Inorg. Chem. 26 (1987) 2205.
[10] S. Lo Schiavo, G. Bruno, P. Zanello, F. Laschi, P. Piraino, Inorg. Chem. 36 (1997) 1004.
[11] M.P. Doyle, R. Pieters, S.F. Martin, R.E. Austin, C.J. Oalmann, P. Muller, J. Am. Chem. Soc. 113 (1991) 1423.
[12] M.P. Doyle, M. Protopopova, P. Muller, D. Ene, E. Shapiro, J. Am. Chem. Soc. 116 (1994) 8492.
[13] M.P. Doyle, A. Van Oeverne, L.J. Vestrum, M.N. Protopopova, T.W. Clayton, J. Am. Chem. Soc. 113 (1991) 8982.
[14] M.P. Doyle, T. Ren, Prog. Inorg. Chem. 49 (2001) 113.
[15] V. Fimiani, T. Ainis, A. Cavallaro, P. Piraino, J. Chemother. 2 (1990) 319.
[16] (a) F.A. Cotton, L.M. Daniels, C. Lin, C.A. Murrillo, J. Am. Chem. Soc. 121 (1999) 4538;
(b) S. Lo Schiavo, S. Serroni, F. Puntoriero, G. Tresoldi, P. Piraino, Eur. J. Inorg. Chem. (2002) 79;
(c) S. Lo Schiavo, S. Serroni, F. Puntoriero, G. Tresoldi, P. Piraino, Eur. J. Inorg. Chem., in press.
[17] E. Rotondo, G. Bruno, F. Nicolò, S. Lo Schiavo, P. Piraino, Inorg. Chem. 30 (1991) 1195.
[18] F.A. Cotton, T.R. Felthouse, Inorg. Chem. 20 (1981) 600.
[19] A. Tiripicchio, M. Tiripicchio Camellini, R. Uson, L.A. Oro, M.A. Ciriano, F. Viguri, J. Chem. Soc., Dalton Trans. (1984) 125.
[20] J.P. Collin, A. Jouaiti, J.P. Sauvage, W.K. Kaska, M.A. Mcloughlin, N.L. Keder, W. Harrison, G.D. Stuky, Inorg. Chem. 29 (1990) 2238.
[21] S. Lo Schiavo, M.S. Sinicropi, G. Tresoldi, C.G. Arena, P. Piraino, J. Chem. Soc., Dalton Trans. (1994) 1517.
[22] N.B. Behrens, G.M. Carrera, D.M.L. Goodgame, A.S. Lawrence, D.J. Williams, Inorg. Chim. Acta 102 (1985) 173.
[23] F.H. Allen, J.E. Davies, J.J. Galloy, O. Johnson, O. Kennard, C.F. Macrae, E.M. Mitchell, G.F. Mitchell, J.M. Smith, D.G. Watson, J. Chem. Inf. Comp. Sci. 31 (1991) 187.
[24] W.S. Sheldrick, M. Mintert, Inorg. Chim. Acta 219 (1994) 23.
[25] G.R. Newkome, S.J. Garbis, V.K. Majestic, F.R. Fronczek, G. Chiari, J. Org. Chem. 46 (1981) 833.
[26] F.A. Cotton, Y. Kim, Eur. J. Solid State Inorg. Chem. 31 (1994) 525.
[27] A. Mangini, M. Colonna, Gazz. Chim. Italiana LXXIII (1943) 323.
[28] R. Diamond, Acta Crystallogr., A 25 (1969) 43.
[29] G. Kopfmann, R. Huber, Acta Crystallogr., A 24 (1968) 348.
[30] G.M. Sheldrick, SHELXL97-2: Program for Crystal Structure Refinement, University of Göttingen, Göttingen, Germany, 1997.
[31] International Tables for X-ray Crystallography, vol C, tables 4.2.6.8 and 6.1.1.4, Kynoch Press, Birmingham, 1992.
[32] M. Nardelli, J. Appl. Chem. 28 (1995) 659 (version locally modified).